

# Study on Microemulsion Polymerization of *N*-Butyl Maleimide

YOU LIANG ZHAO, HUAMING LI, PENGSHENG LIU

College of Chemistry and Chemical Engineering, Xiangtan University, Xiangtan 411105 People's Republic of China

Received 11 May 1999; accepted 14 October 1999

**ABSTRACT:** By using sodium dodecyl sulfate (SDS) as an emulsifier, polymerization of *N*-butyl maleimide (NBMI) was carried out in ternary oil-in-water microemulsion, initiated with potassium persulfate (KPS). The kinetics of microemulsion polymerization were measured by dilatometry. The effects of initiator concentration, polymerization temperature, monomer concentration, and emulsifier concentration on polymerization kinetics were investigated. On this basis, the polymerization kinetics were discussed. The experiment result showed that the microemulsion polymerization kinetics of *N*-butyl maleimide were almost consistent with the prediction of the Smith-Ewart theory in conventional emulsion polymerization, except that the emulsifier showed a special effect on polymerization. At the same time, the polymer was characterized by IR, <sup>1</sup>H-NMR, DSC, and TGA. © 2000 John Wiley & Sons, Inc. *J Appl Polym Sci* 77: 805–809, 2000

**Key words:** oil-in-water microemulsion; *N*-butyl maleimide; microemulsion polymerization; polymerization kinetics

## INTRODUCTION

Both maleimide and bismaleimide are important organic compounds that are widely used in polymer synthesis, medical materials, agricultural chemistry, and dye industry.<sup>1</sup> After polymerization, their polymers are among the most important resins in industry because of their tractability, high thermal stability, high durability, good water resistance, fire resistance, radiation resistance, and relatively low cost.<sup>2–4</sup> Moreover, their copolymers are used as a new-type polymer heat-resistant modifier in the 1990s due to their good compatibility with all sorts of thermoplastic resins.<sup>5</sup>

The microemulsion polymerization has attracted wide attentions since it was firstly reported by Stoffer and Bone in 1980,<sup>6</sup> because

this technology has many advantages such as rapid polymerization rate and high polymer molecular weight. Furthermore, compared with conventional emulsion polymerization, the polymers resulting from microemulsion polymerization possess less particle size and narrower molecular distribution. So far, many researches on microemulsion polymerization have been carried out, but the microemulsion polymerization of maleimide and its derivatives has not been reported. Recently, some oil-soluble monomers have been successfully polymerized in ternary microemulsion systems.<sup>7–10</sup>

In this study, sodium dodecyl sulfate (SDS) was used as the emulsifier, and the O/W ternary microemulsion containing *N*-butyl maleimide (NBMI) was firstly prepared. The microemulsion was polymerized in dilatometer with potassium persulfate (KPS) as the initiator. The polymerization kinetics were investigated in detail, and the resulting polymer was characterized by IR, <sup>1</sup>H-NMR, DSC, and TGA as well. The success of this

---

Correspondence to: YouLiang Zhao.

*Journal of Applied Polymer Science*, Vol. 77, 805–809 (2000)  
© 2000 John Wiley & Sons, Inc.

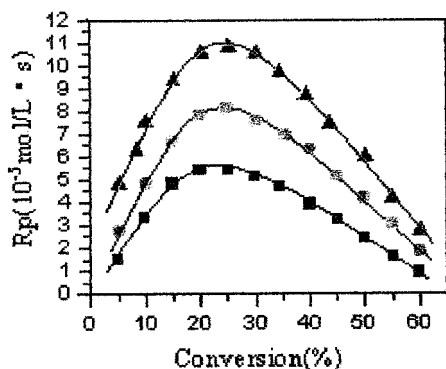


**Figure 1** Polymerization vs. conversion at different KPS concentrations. [NBMI] = 0.35M, [SDS] = 0.35M,  $T = 70^{\circ}\text{C}$ ; KPS (mmol/L): (1) 1.75 ( $\blacktriangle$ ); (2) 0.88 ( $\bullet$ ); (3) 0.49 ( $\blacksquare$ ).

attempt exhibits a new access to synthesize polymers of maleimide and its derivatives. Moreover, the method proposed herein can also be potentially used for the preparation of their copolymers.

## EXPERIMENTAL

### Materials and Instruments

KPS, obtained from the Beijing Chemical Reagent Factory, was recrystallized twice from distilled-deionized water. NBMI was synthesized and purified according to the method described in the literature.<sup>11</sup> All the other reagents used in this study were of analytical grade, and used without further purification.

Infrared (IR) spectra were recorded with a Perkin-Elmer 1710 instrument. The  $^1\text{H-NMR}$  spectra

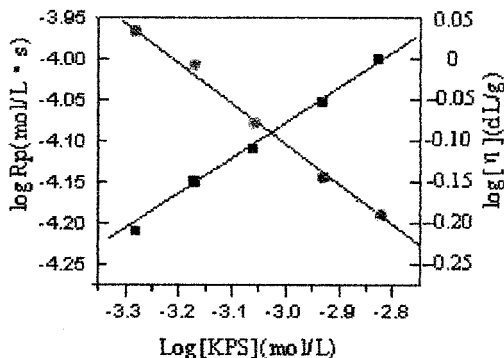


**Figure 2** Effect of KPS on polymerization rate ( $\blacksquare$ ) and intrinsic viscosity ( $\bullet$ ). [NBMI] = 0.35M, [SDS] = 0.35M,  $T = 70^{\circ}\text{C}$ .

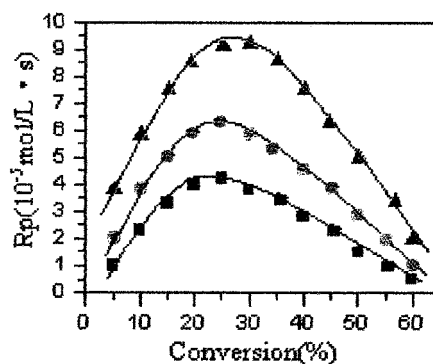


**Figure 3** Polymerization rate vs. conversion at different monomer concentrations. [KPS] = 1.25 mM, [SDS] = 0.35M,  $T = 70^{\circ}\text{C}$ . NBMI (mol/L): (1) 0.35 ( $\blacktriangle$ ); (2) 0.25 ( $\bullet$ ); (3) 0.18 ( $\blacksquare$ ).

was obtained on a varian DRX-400 spectrometer. Differential scanning calorimetry (DSC) was carried out on a Perkin-Elmer Model DSC-7, using scanning rate of 10 K/min in nitrogen. Thermal stability of polymer (TGA) was determined on a Perkin-Elmer TG-40 thermogravimetric system in the temperature range of 30–250°C. The intrinsic viscosity of the polymerizing solution was measured by a Ubbelodhe viscosimeter at 30°C, using chloroform as the solvent.

### Preparation of SDS/NBMI/H<sub>2</sub>O Ternary Microemulsion

NBMI was added to the aqueous solution of sodium dodecyl surfate in a capped ampoule. The contents of the ampoule were agitated at room temperature by means of a glass stirred bar for about 30 min. It was then stored for 2 h to attain equilibrium.

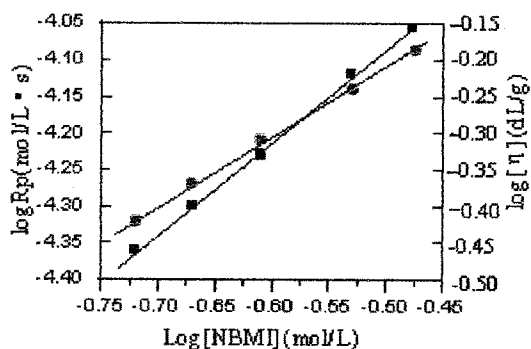


**Figure 4** Effect of NBMI on polymerization rate ( $\blacksquare$ ) and intrinsic viscosity ( $\bullet$ ). [KPS] = 1.25 mM, [SDS] = 0.35M,  $T = 70^{\circ}\text{C}$ .

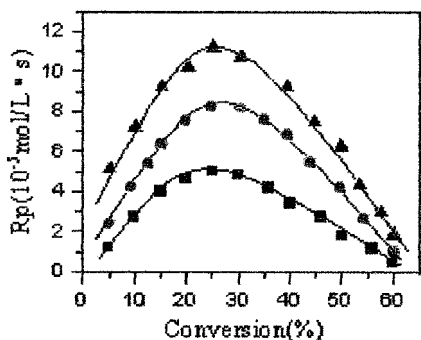


**Figure 5** Polymerization Rate vs. conversion at different monomer concentrations. [KPS] = 1.25 mM, [NBMI] = 0.35M,  $T = 70^{\circ}\text{C}$ . SDS (mol/L): (1) 0.62 ( $\blacktriangle$ ); (2) 0.42 ( $\bullet$ ); (3) 0.29 ( $\blacksquare$ ).

**Microemulsion Polymerization of NBMI**

Polymerization of NBMI was carried out in a glass dilatometer. Prior to polymerization, the microemulsion with the requisite amount of KPS were degassed twice with water pump to remove oxygen. Then the microemulsion was introduced directly into a 35-mL dilatometer, which was placed in a water bath to polymerize at  $70^{\circ}\text{C}$ . The change of liquid level in the capillary of the dilatometer was recorded as a function of time, and the fractional conversion was determined from the volume change. The polymerization rate was then acquired from the differential curve of conversion vs. time.

**Purification of Poly(*N*-butyl maleimide)**

After polymerization, the microemulsion was poured into a large quantity of methanol. The resulting polymer was dissolved in chloroform, then reprecipitated with methanol to remove

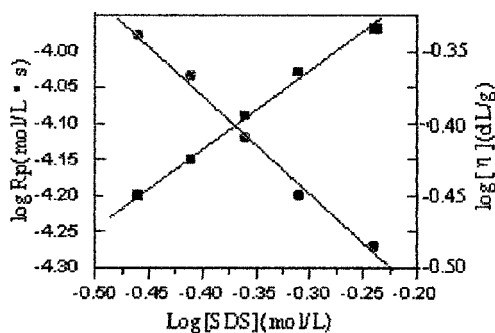


**Figure 6** Effect of emulsifier on polymerization rate ( $\blacksquare$ ) and intrinsic viscosity ( $\bullet$ ). [KPS] = 1.25 mM, [NBMI] = 0.25M,  $T = 70^{\circ}\text{C}$ .

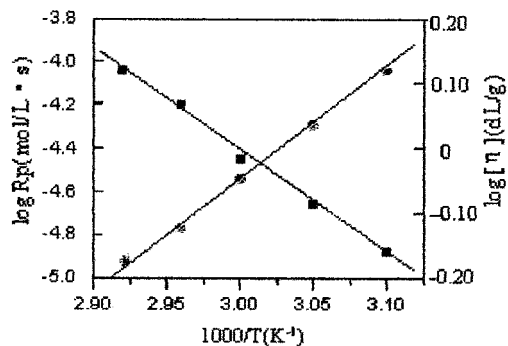


**Figure 7** Effect of polymerization temperature on polymerization rate ( $\blacksquare$ ) and intrinsic viscosity ( $\bullet$ ). [KPS] = 1.25 mM, [SDS] = 0.35M, [NBMI] = 0.35M.

emulsifier completely. After that, the polymer was dried overnight in vacuum.

**RESULTS AND DISCUSSION**

**Study on Microemulsion Polymerization Kinetics**

**Effect of KPS Concentration**

Polymerization rates at different KPS concentrations were plotted against the conversion in Figure 1. There was no apparent plateau of polymerization rate; moreover, the maximum polymerization rate appeared when the conversion reached 20–30%, which is different from that in conventional emulsion polymerization. It is shown in

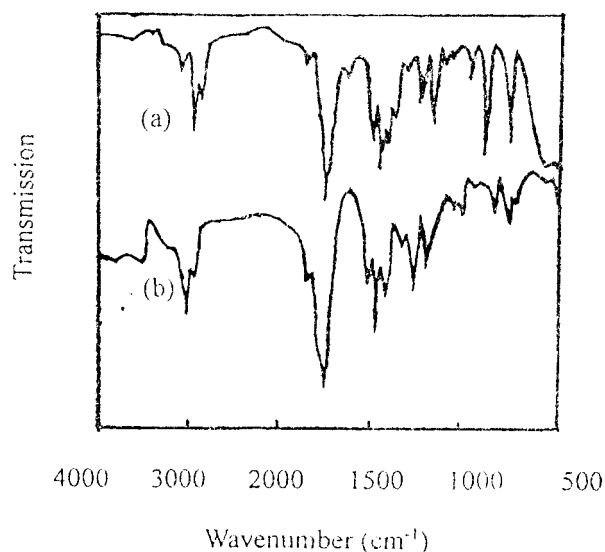


**Figure 8** IR spectra of NBMI (spectrum a) and PN-BMI (spectrum b).

**Table I** Wave Numbers of IR Spectra of NBMI and PNBMI ( $\text{cm}^{-1}$ )

Sample	Imide Structure				C—CH <sub>3</sub>			C=C		
NBMI	1790	1707	1409	1183	697	1445	1370	3100	1591	831
PNBMI	1776	1697	1407	1193	660	1442	1356			

Figure 2 that  $R_p \propto [\text{KPS}]^{0.45}$ ,  $[\eta] \propto [\text{KPS}]^{-0.48}$ . The result is quite consistent with that predicted from the Smith-Ewart Case 2 hypothesis in conventional emulsion polymerization.

#### Effect of Monomer Concentration

As shown in Figure 3, there was no apparent plateau of polymerization rate also. Polymerization rate and intrinsic viscosity increased with the increasing of monomer concentration, which is almost consistent with the predicting result. Figure 4 shows that the dependencies of  $R_p$  and  $[\eta]$  on monomer concentration are 1.24 and 0.88 powers, respectively.

#### Effect of Emulsifier Concentration

The polymerization rate vs. different emulsifier contents is shown in Figure 5. As shown in Figure 6, the dependencies of 1.14 and  $-0.75$  powers are obtained for  $R_p$  and  $[\eta]$  vs. emulsifier concentration, respectively. The result shows that when the emulsifier concentration increases, the polymerization rate increases, while the intrinsic viscosity decreases. It is obvious that the result is different from that predicted by Smith-Ewart theory, like other microemulsion polymerization systems.<sup>8</sup>

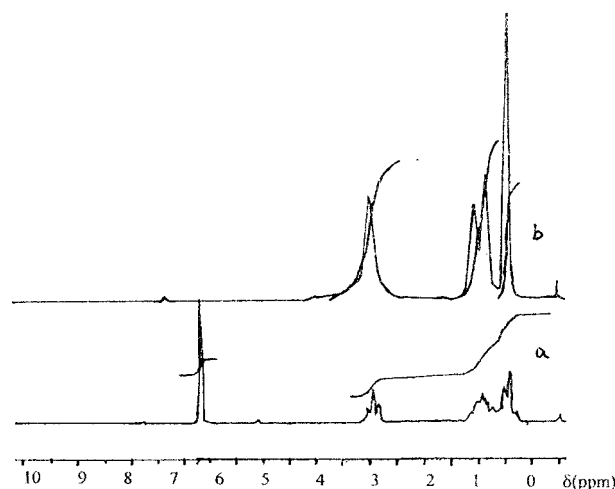


**Figure 9**  $^1\text{H-NMR}$  spectra of NBMI (a) and PNBMI (b).

#### Effect of Polymerization Temperature

The effect of polymerization temperature was studied by initiating the same microemulsion at different temperatures. As expected, the increasing temperature leads to increasing polymerization rate and lower intrinsic viscosity. From the Arrhenius plot of  $\log R_p$  and  $\log[\eta]$  vs.  $1/T$  (Fig. 7), the overall activation energy  $E_{R_p}$  and  $E_\eta$  are 89.2 and  $-29.8$  kJ/mol, respectively.

#### Discussion on Polymerization Kinetics

When the microemulsion of *N*-butyl maleimide was polymerized with potassium persulfate as the initiator, the polymerization kinetics were almost consistent with the Smith-Ewart theory in conventional emulsion polymerization, but the emulsifier showed special effect on polymerization.

It is well known that in microemulsion the disperse phase consists of small droplets with diameters smaller than 100 nm; the number of monomer droplets are very large, so the principal loci of microemulsion polymerization are monomer droplets and micelles. When the emulsifier concentration increases, the emulsifier layer outside the monomer droplets becomes thicker, which makes it more difficult for free radicals diffusing into living polymer particles; thus, they

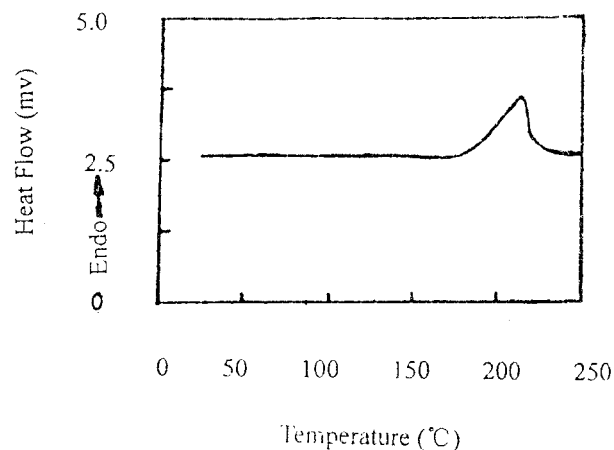


**Figure 10** DSC Curve of PNBMI.

**Table II**  $^1\text{H-NMR}$  Data of NBMI and PNBMI (300 MHz,  $\text{CDCl}_3$ , ppm)

Sample	$-\text{CH}=\text{CH}-$	$-\text{CH}-\text{CH}-$	$-\text{CH}_2-\text{CH}_2-\text{CH}_3$	$-\text{CH}_2-\text{N}$	$-\text{CH}_3$
NBMI	6.66 (s,2H)		1.43 (m, 4H)	3.44 (t,2H)	0.92 (t,3H)
PNBMI		3.04 (s,4H)	1.27 (s, 2H),1.49 (s,2H)	3.04 (s,4H)	0.89 (s,3H)

are liable to transfer to the emulsifier so as to terminate. As a result, the total radical concentration increases, the probability of bimolecular termination reduces, while the probability of chain transfer termination increases. Therefore, the increasing emulsifier concentration can lead to increasing polymerization rate and lower polymer molecular weight.

### Characterization of PNBMI

The polymer of NBMI (PNBMI) was characterized by IR,  $^1\text{H-NMR}$ , DSC, and TGA. The characteristic absorption bands in the IR spectra and their assignments are listed in Table I. The typical IR spectra of NBMI and its polymer are presented in Figure 9 as an example.

As can be seen in Figure 8, the IR spectrum of PNBMI (spectrum b) shows some differences from that of NBMI (spectrum a). The characteristic absorption bands of imide structure at  $1697\text{ cm}^{-1}$ ,  $1193\text{ cm}^{-1}$ , and  $660\text{ cm}^{-1}$  in spectrum b are broader than the corresponding bands in spectrum a. Besides, the characteristic absorption bands of the  $\text{C}=\text{C}$  linkage at  $3100\text{ cm}^{-1}$ ,  $1591\text{ cm}^{-1}$ , and  $831\text{ cm}^{-1}$  entirely disappear in spectrum b.

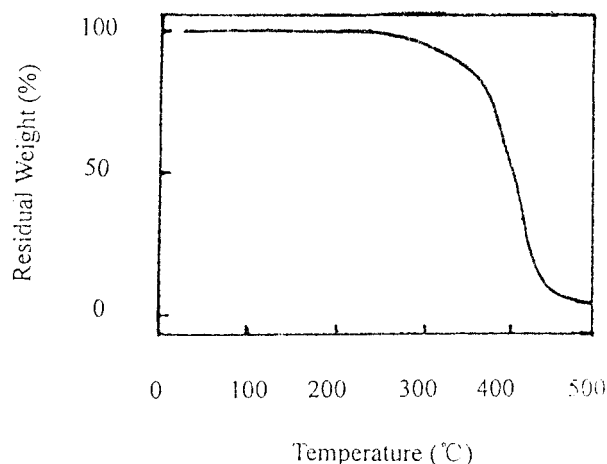
**Figure 11** TGA Curve of PNBMI.

Figure 9 shows the  $^1\text{H-NMR}$  spectra of NBMI and PNBMI. From Figure 9, we can see that there are some differences between spectrum a and spectrum b. The chemical shifts and their corresponding protons are shown in Table II.

To examine the thermal stability of PNBMI, differential scanning calorimetry and thermogravimetric analysis were carried out in a nitrogen stream. The resulting DSC and TGA curves are shown in Figures 10 and 11, respectively.

It is found that the glass transition temperature ( $T_g$ ) of PNBMI is  $183^\circ\text{C}$ , and the initial decomposition temperature is  $296^\circ\text{C}$ , which is similar to the literature values reported for poly(*N*-butyl maleimide).<sup>12</sup> The good heat-resistant properties of the polymer are determined by its special molecular structure. The existence of imide-ring structure restricts the rotation of  $\text{C}-\text{C}$  bond, which makes the macromolecular rigidity increase. Consequently, the thermal stability of the polymer is relatively high.

### REFERENCES

- Inagaki, T.; Takayanagi, Y.; Narita, T. JP 1988, 63, 122, 666.
- Yuan, Q. L.; Huang, F. H.; Jiao, Y. S. J Appl Polym Sci 1996, 62, 459.
- Qiu, W. L.; Zeng, F. X.; Lu, L. D., et al. J Appl Polym Sci 1996, 59, 1551.
- Wang, X.; Chen, D. Y.; Ma, W., et al. J Appl Polym Sci 1999, 71, 665.
- Shan, G. R.; Wen, Z. X.; Huang, Z. M., et al. Polym Mater 1996, 2, 36.
- Stoffer, J. O.; Bone, T. J Polym Sci Polym Chem 1980, 18, 2641.
- Guo, R.; Song, G. P.; Qiang, J. P. Chem J Chin U 1997, 12, 2073.
- Xu, X. L.; Zhang, Z. C.; Zhang, M. W., et al. Chem J Chin U 1997, 9, 1546.
- Wei-Hua, M.; Jones, F. N.; Fu, S. Polym Bull 1998, 40, 749.
- Xu, X. L.; Ge, X. W.; Zhang, Z. C., et al. Polymer 1998, 39, 5321.
- Schwartz, A. L.; Lerner, L. M. J Org Chem 1974, 39, 21.
- Takayuki, O.; Akikazu, M.; Toru, K., et al. Polym Bull 1990, 23, 43.